Size effects in the torsion of thin metal wires

Martín I Idiart[1,2] **and Norman A Fleck**[1]

[1] Centre for Micromechanics, Department of Engineering, University of Cambridge, Trumpington Street, Cambridge CB2 1PZ, U.K.
[2] Área Departamental Aeronáutica, Facultad de Ingeniería, Universidad Nacional de La Plata, Calles 1 y 47, La Plata B1900TAG, Argentina.

E-mail: mii23@cam.ac.uk

Abstract. The elasto-plastic torsional response of a thin metal wire is analyzed using the phenomenological flow theory of strain gradient plasticity proposed by Fleck and Willis (Part I: *J. Mech. Phys. Solids* 57 (2009) 161, Part II: submitted). Numerical results are obtained via minimum principles, and closed-form expressions are derived in the limit of vanishing elasticity. An elevation of both initial yield and hardening rate is predicted with decreasing wire diameter. The role of the stored energy of cold work is investigated, and its implications for kinematic hardening are discussed.

Submitted to: *Modelling Simulation Mater. Sci. Eng.*

1. Introduction

Fleck et al. [1] performed tension experiments and torsion experiments on pure copper wires whose diameters ranged from 12μm to 170μm. They observed a strong size effect in torsion whereby the flow stress of the thinnest wires deep in the plastic range was about three times higher than that of the thickest wires. In contrast, no size effects were observed in the tension tests. More recent torsion experiments on 10-50μm copper wires by Ehrler et al. [2] show comparable size effects at incipient yielding. This elevation of flow stress with decreasing size can be attributed to the spatial gradients of plastic strain, which lead to enhanced hardening through the storage of geometrically-necessary dislocations [1]. Phenomenological strain-gradient theories of isotropic plasticity represent a relatively simple engineering approach to modelling such size effects. In this paper, the torsion of thin metal wires is analyzed by means of a strain-gradient plasticity theory recently proposed by Fleck and Willis [3, 4]. This incremental higher-order theory draws upon earlier work by Fleck and Hutchinson [6] and Gudmundson [5]; it assumes associated plastic flow and possesses a convex yield surface. Positive dissipation is ensured, and uniqueness and extremum principles can be stated. In the remainder of this section we summarize the field equations and constitutive assumptions.

The theory postulates an internal work statement in terms of the elastic and plastic strain rates $\dot{\varepsilon}_{ij}^{EL}$ and $\dot{\varepsilon}_{ij}^{PL}$, along with the spatial gradient of plastic strain rate $\dot{\varepsilon}_{ij,k}^{PL}$. The virtual work statement reads

$$\int_V \left[\sigma_{ij}\dot{\varepsilon}_{ij}^{EL} + q_{ij}\dot{\varepsilon}_{ij}^{PL} + \tau_{ijk}\dot{\varepsilon}_{ij,k}^{PL}\right] dV = \int_S \left[T_i\dot{u}_i + t_{ij}\dot{\varepsilon}_{ij}^{PL}\right] dS, \tag{1}$$

thereby defining work-conjugate stress quantities σ_{ij}, q_{ij} and τ_{ijk} in the domain V occupied by the solid, and the surface tractions T_i and t_{ij} on the external boundary S of the solid. The strain rates satisfy the standard kinematic relations

$$\dot{\varepsilon}_{ij} = \frac{1}{2}\left(\dot{u}_{i,j} + \dot{u}_{j,i}\right), \quad \dot{\varepsilon}_{ij} = \dot{\varepsilon}_{ij}^{EL} + \dot{\varepsilon}_{ij}^{PL}, \quad \dot{\varepsilon}_{ii}^{PL} = 0, \tag{2}$$

where $\dot{u}_i$ is the displacement rate. Balance laws for the stress quantities follow directly from the principle of virtual work:

$$\sigma_{ij,j} = 0 \qquad \text{and} \quad q_{ij} - \tau_{ijk,k} = \sigma'_{ij} \quad \text{in } V, \tag{3}$$

$$\sigma_{ij}n_j = T_i \quad \text{and} \quad \tau_{ijk}n_k = t_{ij} \qquad \text{on } S, \tag{4}$$

and $\sigma_{ij} = \sigma_{ji}$, $q_{ij} = q_{ji}$, $q_{ii} = 0$, $\tau_{ijk} = \tau_{jik}$, $\tau_{iik} = 0$. In these expressions, σ'_{ij} is the deviatoric Cauchy stress, and the normal n_i is directed outwards.

The solid is assumed to be isotropic, incompressible and elasto-plastic. The elastic behavior is characterized by

$$\sigma'_{ij} = \frac{\partial U}{\partial \varepsilon_{ij}^{EL}} = \frac{2}{3}E\varepsilon_{ij}^{EL}, \tag{5}$$

where $U(\varepsilon_{ij}^{EL})$ is the internal energy density of the solid and E denotes the Young's modulus.

The plastic behavior is characterized in terms of $\dot{\varepsilon}^{PL}_{ij}$ and its spatial gradient $\dot{\varepsilon}^{PL}_{ij,k}$. In the remainder of this section, and in Sections 2 and 3, plastic work is taken to be purely dissipative in nature. In the final section, kinematic hardening is addressed, and the internal energy is taken to depend on ε^{PL}_{ij} and $\varepsilon^{PL}_{ij,k}$. Three material length-scales can enter on dimensional grounds [6]; we restrict attention to the simplest model, containing a single material length-scale ℓ. Following Fleck and Hutchinson [7], plastic dissipation is assumed to depend on effective measures of plastic strain rate and stress of the form

$$\dot{E}_P = \sqrt{\frac{2}{3}} \left[\left(\dot{\varepsilon}^{PL}_{ij} \dot{\varepsilon}^{PL}_{ij} \right)^{\frac{\mu}{2}} + \left(\ell^2 \dot{\varepsilon}^{PL}_{ij,k} \dot{\varepsilon}^{PL}_{ij,k} \right)^{\frac{\mu}{2}} \right]^{\frac{1}{\mu}}, \tag{6}$$

$$\Sigma = \sqrt{\frac{3}{2}} \left[(q_{ij} q_{ij})^{\frac{\mu}{2(\mu-1)}} + (\ell^{-2} \tau_{ijk} \tau_{ijk})^{\frac{\mu}{2(\mu-1)}} \right]^{\frac{\mu-1}{\mu}}, \tag{7}$$

where the exponent μ is an additional material parameter. The first term inside brackets in (6) is attributed to dissipation caused by the motion of statistically-stored dislocations, while the second term is attributed to geometrically-necessary dislocations [8]. The exponent μ parametrizes different ways of combining these two contributions. When the strain gradients are small, the measures reduce to the conventional von Mises plastic strain rate and stress, regardless of the value of μ.

The plastic flow rule is conveniently expressed in terms of 20-dimensional stress and strain-rate vectors

$$\mathcal{S}_I = \left(q_{ij},\ \ell^{-1} \tau_{ijk} \right), \quad \dot{\mathcal{E}}_I = \left(\dot{\varepsilon}^{PL}_{ij},\ \ell \dot{\varepsilon}^{PL}_{ij,k} \right), \tag{8}$$

$I = 1, ..., 20$. We shall adopt the convention that a repeated subscript I denotes summation over the corresponding lower-case indices. In order to guarantee positive dissipation, associative plastic flow is assumed, whereby the strain-rate vector $\dot{\mathcal{E}}_I$ is taken to be normal to a convex yield surface defined in the space of stress vectors $\mathcal{S}_I$ by

$$f(\mathcal{S}_I; E_P) = \Sigma - \sigma_y(E_P) = 0, \tag{9}$$

where $\sigma_y(E_P)$ is the uniaxial flow strength of the material, evaluated at the accumulated effective plastic strain $E_P = \int \dot{E}_P dt$. The strength is thus elevated by the presence of plastic strain gradients. The flow rule is then given by

$$\dot{\mathcal{E}}_I = \begin{cases} \dfrac{\dot{\Sigma}}{h} \dfrac{\partial \Sigma}{\partial \mathcal{S}_I} & \text{if } \Sigma = \sigma_y(E_P) \text{ and } \dot{\Sigma} > 0, \\ 0 & \text{otherwise,} \end{cases} \tag{10}$$

where $h = \sigma_y'(E_P)$ is the hardening rate of the material and $\dot{\Sigma} = \dot{\mathcal{S}}_I \partial \Sigma / \partial \mathcal{S}_I$ is the projection of the generalized stress rate on the yield surface normal. During plastic loading, $\dot{\Sigma} > 0$ and continued yield implies the consistency relation $\dot{\Sigma} = h \dot{E}_P$. The dissipation rate is thus $\mathcal{S}_I \dot{\mathcal{E}}_I = \sigma_y \dot{E}_P \geq 0$, as required by thermodynamics.

In the absence of strain-gradient effects, the flow rule (10) demands vanishing higher-order stresses τ_{ijk}, the equilibrium equation $(3)_2$ reduces to $q_{ij} = \sigma'_{ij}$, and conventional von Mises plasticity is recovered.

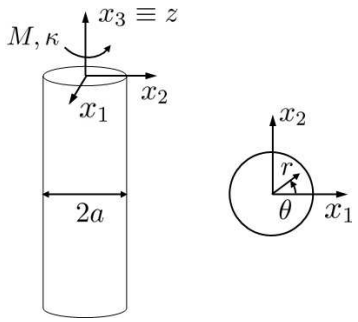

Figure 1. Schematic of wire under torsion and coordinate systems.

2. Monotonic torsion of elasto-plastic thin wires

The wire is idealized as a circular cylindrical bar of diameter $2a$ subjected to monotonic torsion. The cylindrical coordinate system shown in fig. 1 is employed throughout. Following Fleck et al. [1], it is assumed that the twist is imposed via displacement boundary conditions at the ends of the wire, and traction-free boundary conditions are imposed on the periphery of the wire: $T_i^0 = t_{ij}^0 = 0$ at $r = a$. The displacement field is the same as in classical torsion; in polar coordinates, the only non-zero components of the total and plastic strain-rate tensors can be written as

$$\dot{\varepsilon}_{\theta z} = \dot{\varepsilon}_{z\theta} = \frac{\dot{\kappa}}{2} r \quad \text{and} \quad \dot{\varepsilon}_{\theta z}^{PL} = \dot{\varepsilon}_{z\theta}^{PL} = \frac{\sqrt{3}}{2} \dot{\varepsilon}_P(r), \tag{11}$$

where $\dot{\kappa}$ is the rate of twist per unit length, and $\dot{\varepsilon}_P$ is the standard von Mises plastic strain rate.

It is not clear at this point what value of μ should be adopted in the effective measures (6) and (7), see for instance [7, 9]. Most studies adopt the value $\mu = 2$, primarily because it leads to robust numerical implementations of the model. This value is also adopted here –the more general case will be considered in the next section. The effective plastic strain rate (6) is thus

$$\dot{E}_P = \sqrt{\dot{\varepsilon}_P^2 + \ell^2 \left[(\dot{\varepsilon}_P')^2 + \left(\dot{\varepsilon}_P / r \right)^2 \right]}, \tag{12}$$

where $(\cdot)' \equiv d(\cdot)/dr$. The uniaxial tensile behavior of the material is characterized by a Ramberg-Osgood law

$$\frac{\varepsilon}{\varepsilon_0} = \frac{\sigma}{\sigma_0} + \left(\frac{\sigma}{\sigma_0} \right)^n, \tag{13}$$

where $\varepsilon_0 = \sigma_0 / E$, σ_0 is a flow stress, and $n = 1/N$ is a hardening exponent. For this choice, the strength of the solid is $\sigma_y(E_P) = (E_P/\varepsilon_0)^N \sigma_0$ and the hardening rate is $h(E_P) = (E_P/\varepsilon_0)^{N-1} NE$. Upon monotonic loading, plasticity develops from the outset throughout the specimen, so that no elastic-plastic boundary is present.

Given the current plastic state, the incremental boundary-value problem for the plastic strain rate field $\dot{\varepsilon}_P(r)$ consists of the compatibility equations (2), the rate forms of the equilibrium equations (3)-(4) and of the elastic constitutive law (5), the plastic

flow rule (10), and the boundary conditions on S. This problem can be recast in the form of two kinematical minimum principles [4]. The first principle yields the unique distribution of generalized stresses $\mathcal{S}_I$, and via (10), the distribution of $\dot{\varepsilon}_P(r)$ up to a multiplicative constant; the constant then follows from the second principle. Thus, we let $\dot{\varepsilon}_P(r) = \dot{\lambda}\hat{\varepsilon}_P(r)$, where $\hat{\varepsilon}_P(r)$ is a "unit" field such that $(1/a)\int_0^a \hat{\varepsilon}_P^2 r dr = 1$ and $\hat{\varepsilon}_P(0) = 0$, which minimizes

$$I = \min_{\hat{\varepsilon}_P} \int_0^a \left[\sigma_y(E_P)\hat{E}_P - \sqrt{3}\sigma_{\theta z}\hat{\varepsilon}_P\right] r dr. \tag{14}$$

Here, $\sigma_{\theta z} = 2E(\varepsilon_{\theta z} - \varepsilon_{\theta z}^{PL})/3$ is the Cauchy stress in the current state, and $\hat{E}_P$ is related to $\hat{\varepsilon}_P$ by an expression analogous to (12). The "magnitude" $\dot{\lambda} \geq 0$ then follows from the second minimum principle,

$$\Psi = \min_{\dot{\lambda}} \int_0^a \left[E\left(\frac{\dot{\kappa}}{\sqrt{3}}r - \dot{\lambda}\hat{\varepsilon}_P\right)^2 + h(E_P)\dot{\lambda}^2\hat{E}_P^2\right] r dr, \tag{15}$$

where $\hat{\varepsilon}_P$ is the solution to (14).

The minimization in (15) is straightforward, giving

$$\dot{\lambda} = \frac{E\dot{\kappa}}{\sqrt{3}} \frac{\int_0^a \hat{\varepsilon}_P r^2 dr}{\int_0^a \left[E\hat{\varepsilon}_P^2 + h(E_P)\hat{E}_P^2\right] r dr} \tag{16}$$

or zero if the right-hand side is negative. The minimization in (14), on the other hand, must be carried out numerically. The plastic strain rate $\hat{\varepsilon}_P(r)$ is obtained by finite element discretization of the functional in (14) and subsequent minimization with respect to the nodal amplitudes. Time integration of the rates is then performed by means of a forward-Euler scheme. Details of the numerical implementation have been given in [9].

Finally, the torque Q is defined as the work-conjugate of the twist κ, so that the external work rate is $Q\dot{\kappa}$. At equilibrium, the work statement (1) and the strain-rate field (11) imply that

$$Q = \frac{1}{\dot{\kappa}} \int_V \sigma_{ij}\dot{\varepsilon}_{ij} dV = 2\pi \int_0^a \sigma_{\theta z} r^2 dr. \tag{17}$$

In Fig. 2 we explore the dependence of torsional response on the ratio of material length scale ℓ to wire radius a, for a low hardening exponent ($N = 0.1$) and a high exponent ($N = 0.3$). Plots are shown for the torque versus twist, normalized by $Q_y = (2\pi/3\sqrt{3})\sigma_0 a^3$ and $\kappa_y = \sqrt{3}\varepsilon_0/a$, respectively, for three values of ℓ/a. The case $\ell/a = 0$ corresponds to conventional elasto-plastic wires with no gradient effects. The predictions for both values of N show a strong size effect with increasing ratio ℓ/a, on both incipient yielding and subsequent hardening rate. For example, the flow stress deep in the plastic range is elevated by a factor of ~ 2.5 when ℓ/a is increased from zero to unity. Taking $\ell = 6\mu$m, the strength of 15μm wires is predicted to be twice that of thick wires. This is on the order of strength elevation observed in copper wires [1, 2]. The elastic response predicted by the theory, on the other hand, is independent of wire

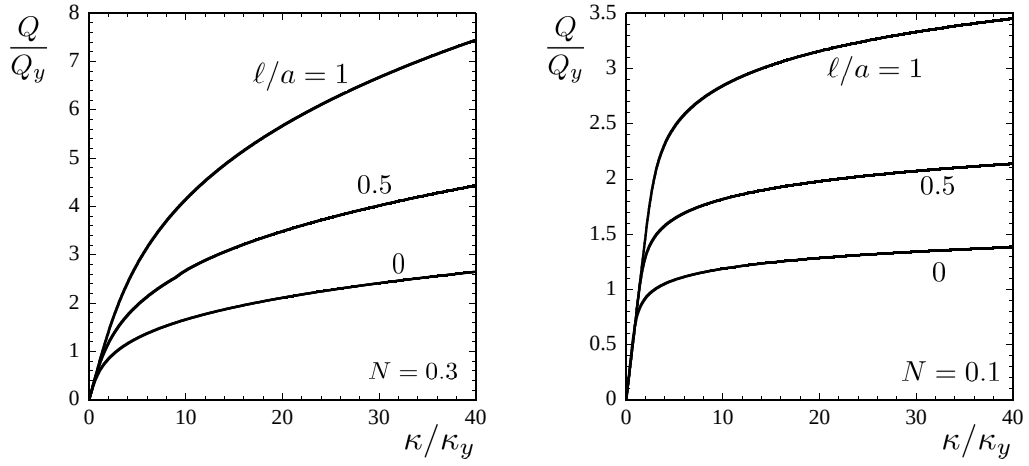

Figure 2. Normalized torque versus twist for elasto-plastic wires of various ratios ℓ/a and strain hardening exponents (a) $N = 0.3$ and (b) $N = 0.1$.

diameter, consistent with experimental observations. This is in contrast to predictions based on micropolar theories (e.g., [10]), which involve gradients of total strain rather than plastic strain, and as a consequence exhibit size effects in the elastic range.

Quantitatively similar results for wires made from a Ramberg-Oswood solid were obtained by Fleck and Hutchinson [6]. These authors considered more general effective measures $\dot{E}_P$ containing three material length scales, but found that only one length scale suffices in wire torsion. Consequently, there is no need to generalize the present approach to three length scales.

3. Rigid-plastic approximation

In the absence of elasticity, the torsional response can be given in closed-form. Formally, this amounts to evaluating the limit $E \to \infty$. In this case, the plastic strain rates $(11)_2$ agree exactly with the total strain rates $(11)_1$, and the effective measure (6) is given by

$$\dot{E}_P = \frac{|\dot{\kappa}|}{\sqrt{3}} \left[r^\mu + (\sqrt{2}\ell)^\mu \right]^{\frac{1}{\mu}} . \tag{18}$$

The work statement (1) and the flow rule (10) imply that the torque is given by

$$Q = \frac{1}{\dot{\kappa}} \int_V \sigma_y(E_P) \dot{E}_P dV = \frac{2\pi}{\sqrt{3}} \int_0^a \sigma_y(E_P) [r^\mu + (\sqrt{2}\ell)^\mu]^{\frac{1}{\mu}} r dr \ \mathrm{sgn}(\dot{\kappa}). \tag{19}$$

Let the plastic response be characterized by a power-law relation

$$\sigma_y(E_P) = \sigma_0 \left(1 + \alpha E_P^N\right), \tag{20}$$

where α is an additional material parameter. This relation has a finite yield strength σ_0. Under monotonic loading, integration of (19) with (20) can be carried out analytically, giving the normalized torque

$$\frac{Q}{Q_y} = f_y\left(\sqrt{2}\ell/a\right) + \alpha f_h\left(\sqrt{2}\ell/a, N\right) \left(\frac{\kappa a}{\sqrt{3}}\right)^N , \tag{21}$$

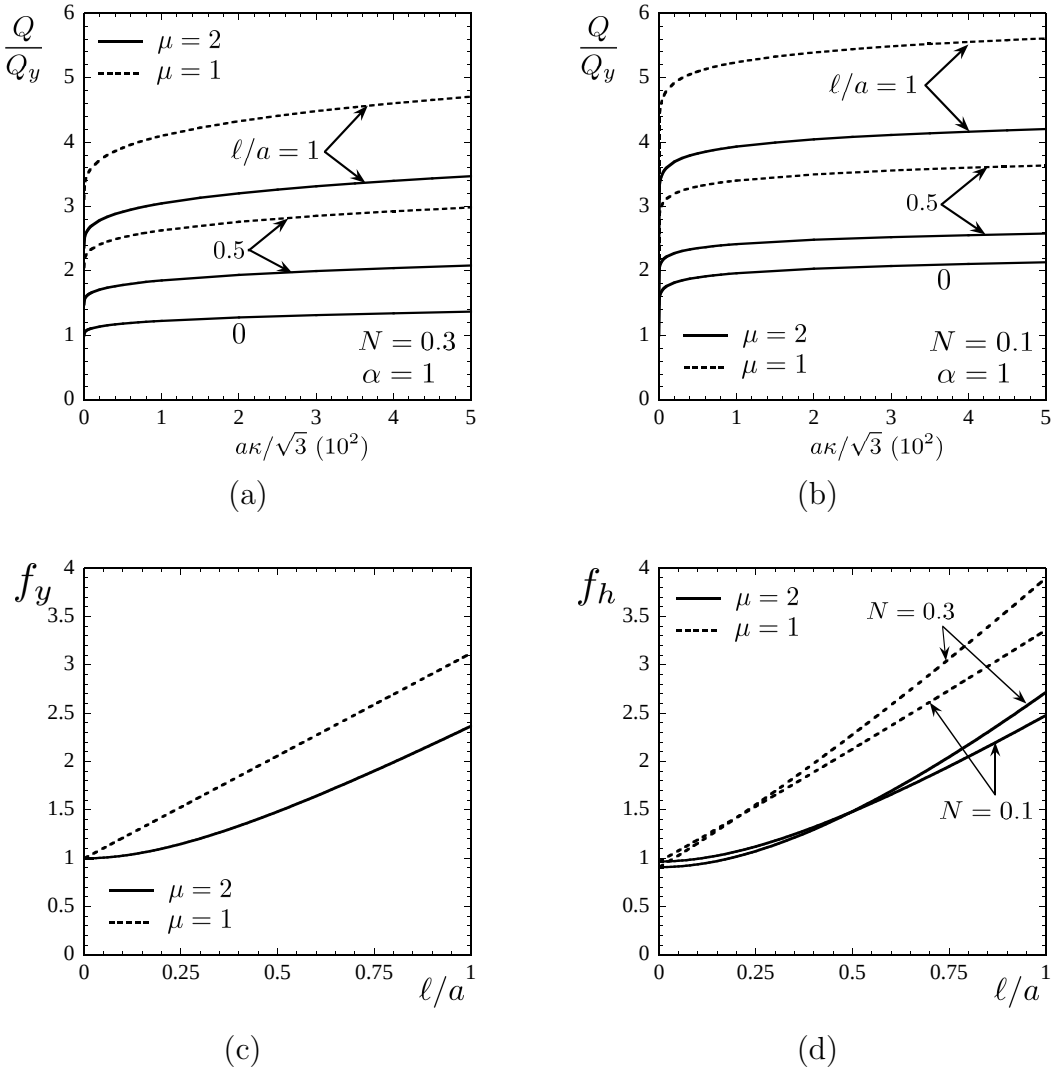

Figure 3. Rigid-plastic wires with $\alpha = 1$ and two values of the exponent μ: normalized torque versus twist for (a) $N = 0.3$ and (b) $N = 0.1$; (c) normalized torque at yield and (d) hardening rate as a function of ℓ/a.

where

$$f_h(\beta, N) = \frac{3}{2}\beta^{N+1}\ {}_2F_1\left(\frac{2}{\mu}, -\frac{N+1}{\mu}; \frac{2+\mu}{\mu}; -\frac{1}{\beta^\mu}\right), \tag{22}$$

and $f_y(\beta) \equiv f_h(\beta, 0)$. In this expression, ${}_2F_1$ denotes the standard hypergeometric series‡. Results for materials exhibiting a pure power-law response $\sigma_y = \sigma_0 E_P^N$ can be readily obtained by neglecting the first term in (21). The rigid-plastic solution (21) captures the general trends for torque versus ℓ/a of elasto-plastic wires, and thus provides a simple and versatile means of extracting material length scales from experimental data.

‡ See, for instance, M. Abramowitz, I.A. Stegun, Handbook of Mathematical Functions with Formulas, Graphs, and Mathematical Tables. Dover, New York, 1972.

For the choice $\mu = 2$ employed in the previous section, the function f_h simplifies to

$$f_h(\beta, N) = \frac{3}{N+3}\left[(1+\beta^2)^{\frac{N+3}{2}} - \beta^{N+3}\right]. \tag{23}$$

Based on dislocation arguments, Fleck and Hutchinson [7] have suggested that the alternative value $\mu = 1$ may be more appropriate (see also [8]). For this choice

$$f_h(\beta, N) = \frac{3}{N+2}\left[(1+\beta)^{N+2} - \frac{(1+\beta)^{N+3} - \beta^{N+3}}{N+3}\right]. \tag{24}$$

Predictions for the normalized torque versus twist, as given by (21), are shown in fig. 3 for $\mu = 1$ and 2, $\alpha = 1$, and for hardening exponents $N = 0.3$ and $N = 0.1$. Strong size effects are observed for both the yield point and the hardening rate. These effects are shown separately in figs. 3c & 3d. The yield point f_y is independent of N, while the hardening rate f_h is relatively insensitive to N in the range considered. The exponent $\mu = 1$ produces stronger effects than $\mu = 2$. This is made explicit by the asymptotic behavior of the torque at yield for small ℓ/a:

$$f_y(\beta) = \begin{cases} 1 + \dfrac{3}{2}\beta^2 + O(\beta^3) & \mu = 2, \\ 1 + \dfrac{3}{2}\beta & \mu = 1, \end{cases} \tag{25}$$

For $\mu = 2$, the strengthening effect is of second order as it scales with $(\ell/a)^2$, while for $\mu = 1$ the effect is linear in ℓ/a. A similar conclusion was drawn by Fleck and Hutchinson [7, 8]. The different trends predicted for the torque with $\mu = 1$ and 2 in the range of small ℓ/a provide an opportunity to establish the choice of μ once sufficiently large sets of experimental data become available.

4. Kinematic hardening

4.1. The role of stored energy of cold work

The above development assumes that plastic work is entirely dissipated. In reality, some portion of plastic work is not dissipated but stored in the plastically deformed material as so-called energy of cold work. This stored energy is related to the evolution of a variety of defects including dislocations [11]. The strain-gradient plasticity framework considered here can account for this effect phenomenologically by postulating an internal energy density U that depends on the plastic strain and its spatial gradient in addition to the elastic strain. In a rigid-plastic analysis of wire torsion the elastic strains are zero, and the work statement (1) reads [4]

$$Q = \frac{1}{\dot\kappa}\int_V \left[\sigma_y(E_P)\dot E_P + \frac{\partial U}{\partial \varepsilon_{ij}^{PL}}\dot\varepsilon_{ij}^{PL} + \frac{\partial U}{\partial \varepsilon_{ij,k}^{PL}}\dot\varepsilon_{ij,k}^{PL}\right] dV. \tag{26}$$

It remains to stipulate a functional form for U. First, we shall follow Gudmundson [5] and assume that U depends only upon $\varepsilon_{ij,k}^{PL}$, and then we shall assume that U depends upon both ε_{ij}^{PL} and $\varepsilon_{ij,k}^{PL}$.

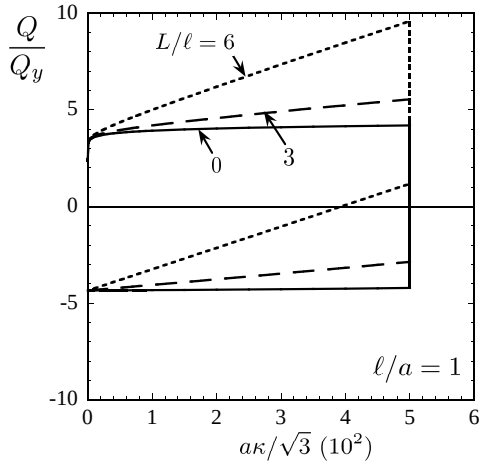

Figure 4. Rigid-plastic wires with quadratic plastic stored energy (27). Normalized torque versus twist for the choice $\mu = 2$, $\alpha = 1$, $N = 0.1$, $\ell/a = 1$, and various ratios of energetic to dissipative length scales L/ℓ.

Gudmundson [5] assumed that the internal energy is a quadratic function of the plastic strain gradient only. Such energy can be written as

$$U(\varepsilon^{PL}_{ij,k}) = \frac{1}{3}\sigma_0 L^2 \varepsilon^{PL}_{ij,k}\varepsilon^{PL}_{ij,k}, \tag{27}$$

where L is an energetic material length-scale distinct from ℓ. Let $\sigma_y(E_P)$ be given by (20). Upon substituting the strain-rate field $(11)_1$ into (26) and integrating we obtain

$$\frac{Q}{Q_y} = \left[f_y\left(\sqrt{2}\ell/a\right) + \alpha f_h\left(\sqrt{2}\ell/a, N\right)\left(\frac{\kappa_t a}{\sqrt{3}}\right)^N \right] \mathrm{sgn}(\dot{\kappa}) + 3\left(\frac{L}{a}\right)^2 \left(\frac{\kappa a}{\sqrt{3}}\right), \tag{28}$$

where $\kappa_t \doteq \int |\dot{\kappa}| dt$, $f_y(\beta) \equiv f_h(\beta, 0)$, and f_h is given by (22). The resulting predictions for torque versus twist are plotted in fig. 4 for the choice $\mu = 2$, $\alpha = 1$, $N = 0.1$, $\ell/a = 1$, and three values of the ratio L/ℓ. Each specimen was loaded until the twist attained the value $(\kappa a/\sqrt{3}) = 0.05$. The twist rate was then reversed in sign and the specimen was reversed loaded until twist attained the value zero. The case $L/\ell = 0$ corresponds to purely dissipative plasticity; it gives a torque-twist curve characterized by the same exponent N as that of the material, and isotropic hardening upon unloading. As the ratio L/ℓ increases, the torque-twist loading curve becomes linear, the hardening rate increases, and a Bauchinger effect, as evidenced by the reverse-yield strength upon unloading, develops. For the larger ratio $L/\ell = 6$, the torque-twist curve shows reverse plasticity at positive torque.

The expression (28) makes explicit the individual contributions of dissipative and energetic higher-order stresses to the torque. As already noted in Section 3, the dissipative stresses give rise to size effects in the initial yielding and the subsequent hardening rate, as given by f_y and f_h in (28), while the energetic stresses introduce size effects only in the hardening rate, as given by the last term in (28). This highlights the importance of dissipative higher-order stresses in rate-independent gradient plasticity;

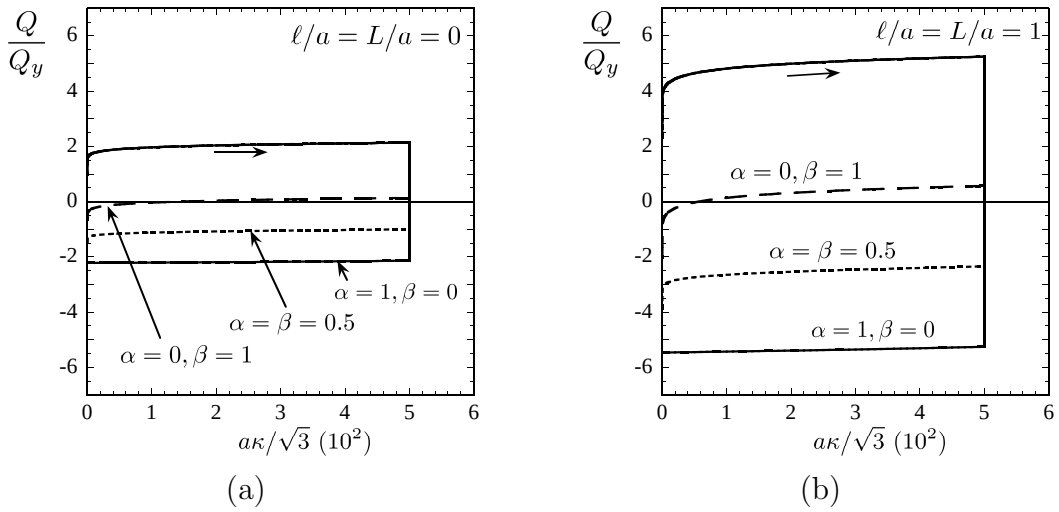

Figure 5. Rigid-plastic wires with power-law plastic stored energy (30). Normalized torque versus twist for the choice $\mu = 2$, $N = 0.1$, and three combinations of α and β. (a) Conventional solid: $\ell/a = L/a = 0$, (b) strain-gradient solid: $\ell/a = L/a = 1$.

gradient plasticity formulations based on purely energetic higher-order stresses (e.g., [5]) cannot predict size-depedent incipient yielding or isotropic hardening.

Typically, the uniaxial response of engineering alloys exhibits kinematic hardening. This effect can be included in the current gradient plasticity formulation by postulating an internal energy U that depends upon plastic strain along with its spatial gradient. We investigate this by introducing an internal energy that depends upon ε_{ij}^{PL} and $\varepsilon_{ij,k}^{PL}$ through the effective measure

$$\overline{E}_P = \sqrt{\frac{2}{3}} \left[(\varepsilon_{ij}^{PL} \varepsilon_{ij}^{PL})^{\frac{\mu}{2}} + (L^2 \varepsilon_{ij,k}^{PL} \varepsilon_{ij,k}^{PL})^{\frac{\mu}{2}} \right]^{\frac{1}{\mu}}. \tag{29}$$

where L is an energetic length scale and μ is the same exponent as that used in (6). In order to preserve the power-law character of the plastic response during forward loading, we take

$$U(\varepsilon_{ij}^{PL}, \varepsilon_{ij,k}^{PL}) = \frac{\beta \sigma_0}{N+1} \overline{E}_P^{N+1}, \tag{30}$$

where β is a non-dimensional material parameter, and N is the same exponent characterizing the hardening in (20). For this choice, the torque (26) is given by

$$\frac{Q}{Q_y} = \left[f_y\left(\sqrt{2}\ell/a\right) + \alpha f_h\left(\sqrt{2}\ell/a, N\right) \left(\frac{\kappa_t a}{\sqrt{3}}\right)^N \right] \mathrm{sgn}(\dot{\kappa}) + \beta f_h\left(\sqrt{2}L/a, N\right) \left|\frac{\kappa a}{\sqrt{3}}\right|^N . \tag{31}$$

The resulting predictions for torque versus twist are plotted in fig. 5 for the choice $\mu = 2$, $N = 0.1$. The cyclic response for a conventional solid with combined isotropic and kinematic hardening is shown in 5a, with $\alpha = \beta = 0.5$. The unloading response is intermmediate between that for purely isotropic hardening ($\alpha = 1$,$\beta = 0$) and that for purely kinematic hardening ($\alpha = 0$,$\beta = 1$). We emphasize that the loading curves are the same for the three choices, but the unloading responses are markedly different. The same

qualitative behavior is demonstrated for the strain-gradient solid with $\ell/a = L/a = 1$, see fig. 5b. Now, the magnitude of torque is amplified by a factor of about two compared to the conventional solid, for the same combination of isotropic and kinematic hardening.

A common practice in experimental works on microbending and microtorsion is to deduce the magnitude of the applied bending moment and torque from the degree of elastic spring-back upon release of the specimen (e.g., [2, 12]), assuming that no reverse plasticity takes place. The above development shows that this assumption may not always hold: reversed plasticity occurs for purely kinematic hardening, for both the conventional solid and the strain-gradient solid.

Acknowledgments

This research is based upon work supported by the Engineering and Physical Sciences Research Council (EPSRC), UK, through a Materials Modelling Programme.

Refereces

[1] Fleck N A, Muller G M, Ashby M F and Hutchinson J W 1994 *Acta Metall. Mater.* **42**, 475–87.
[2] Ehrler B, Bossis R, Joly S, P'ng K M Y, Bushby A J and Dunstan D J, in preparation.
[3] Fleck N A and Willis J R 2009 *J. Mech. Phys. Solids* **57**, 161–77.
[4] Fleck N A and Willis J R, submitted.
[5] Gudmundson P. 2004 *J. Mech. Phys. Solids* **52**, 1379–406.
[6] Fleck N A and Hutchinson J W 2001 *J. Mech. Phys. Solids* **49**, 2245–71.
[7] Fleck N A and Hutchinson J W 1997 *Adv. Appl. Mech.* **33**, 295–361.
[8] Evans A G and Hutchinson J W 2009 *Acta Mater.*, in press.
[9] Idiart M I, Deshpande V S, Fleck N A and Willis J R, submitted.
[10] Grammenoudis P and Tsakmakis C 2005 *Proc. R. Soc. A* **461**, 189-205.
[11] Benzerga A A, Bréchet Y, Needleman A and Van der Giessen, E 2005 *Acta Mater.* **53**, 4765–4779.
[12] Stölken J S and Evans A G 1998 *Acta Mater.* **46**, 5109-5115.